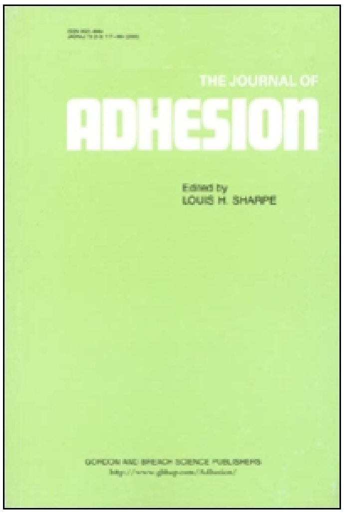

The Journal of Adhesion
Publication details, including instructions for authors and subscription information:
http://www.informaworld.com/smpp/title~content=t713453635

Influence of Composition, Humidity, and Temperature on Chemical Aging in Epoxies: A Local Study of the Interphase with Air

A. Meiser[a]; K. Willstrand[a]; W. Possart[a]
[a] Saarland University, Chair for Adhesion and Interphases in Polymers, Saarbruecken, Germany

To cite this Article Meiser, A. , Willstrand, K. and Possart, W.(2010) 'Influence of Composition, Humidity, and Temperature on Chemical Aging in Epoxies: A Local Study of the Interphase with Air', The Journal of Adhesion, 86: 2, 222 — 243

To link to this Article: DOI: 10.1080/00218460903418352

URL: http://dx.doi.org/10.1080/00218460903418352

The Journal of Adhesion, 86:222–243, 2010

ISSN: 0021-8464 print/1545-5823 online
DOI: 10.1080/00218460903418352

Influence of Composition, Humidity, and Temperature on Chemical Aging in Epoxies: A Local Study of the Interphase with Air

A. Meiser, K. Willstrand, and W. Possart
Saarland University, Chair for Adhesion and Interphases in Polymers, Saarbruecken, Germany

The developing chemical depth profile in an epoxy adhesive bulk (with varying amine content) is monitored during aging by FTIR microspectroscopy on sample cuts prepared with low angle microtomy. Three aging regimes are applied in order to separate the role of temperature and water: dried or moist air (90% rel. humidity) at 60°C and dried air at 120°C for up to 300 days. Quantitative evaluation of the IR spectra shows: thermo-oxidative aging (= dried air) is controlled by the diffusion of atmospheric oxygen. It affects a gradient region of more than 200 μm in depth. At given aging time, the depth profiles depend on temperature, humidity, and on the epoxy-amine ratio. Humidity mainly affects the IR band intensities. The plasticizing effect of water promotes the loss of small network fragments. At 120°C, autoxidation of α*-*CH_2 *at ether and amine groups and the oxidative attack on tertiary amines dominate aging. At 60°C in dried air, these processes proceed only very slowly. In the case of amine excess, aging is extended by the additional oxidation of primary and secondary amines to carbonyls. Carbonyls undergo consecutive reactions, especially in the presence of water. Hence, increasing temperature does not simply accelerate the aging mechanisms but it reduces their selectivity and changes their hierarchy. Thus, the long-term aging behavior at moderate temperatures cannot be predicted safely from accelerated aging tests.*

Keywords: Aging; Chemical depth profiling; Epoxy; FTIR microspectroscopy

Received 19 May 2009; in final form 4 September 2009.

Address correspondence to W. Possart, Saarland University, Chair for Adhesion and Interphases in Polymers, Geb. C6.3, PB 151 150, D-66041 Saarbruecken, Germany. E-mail: w.possart@mx.uni-saarland.de

INTRODUCTION

Chemical aging of polymers limits the durability of structural adhesive bonds and coatings. It depends not only on the substrate and the polymer but also on environmental factors such as humidity, temperature, irradiation, etc. In particular, structural epoxy adhesives have been in the focus of research due to their wide application. Their aging behavior has been studied by various techniques such as FTIR-spectroscopy [1–12], gravimetric analysis [1,3,10,13,14], DSC [2,5–7,15], XPS [10,14], or mass spectroscopy [1,11,12]. The applied aging conditions vary broadly from thermo-oxidation at moderate (60°C) [5,7,15] or elevated temperature (100–250°C) [1–3,13,14] and photo-oxidation [1,2,9–12] to humid or environmental aging conditions at moderate temperatures [4–6]. In any case, FTIR investigations [1,2,4,11,12] show the rise of new IR bands at 1660–1670 cm^{-1} and 1720–1735 cm^{-1} in a region close to the sample surface. The bands are explained by amide and carbonyl formation due to radical oxidation mechanisms initiated by the elevated temperature or UV irradiation [1,2,4,11,12]. Also, backbone scissions are held responsible for the observed decrease in glass transition temperature [2]. At moderate temperature of 60°C, similar bands develop under dry conditions [7]. Upon immersion in water, only one new band at 1660 cm^{-1} is found [6]. These chemical modifications at 60°C are reported to result from the oxidation of residual secondary amines in the network [15]. Thus, the interplay of irradiation, temperature, and humidity is complex, and its effect on chemical aging mechanisms is not completely understood yet.

In this paper, the chemical processes within an epoxy system with varying hardener content are studied during aging under different environmental conditions in order to consider two aspects: first, the influence of residual functional groups within the polymer on the degradation mechanisms is studied by varying the hardener content. Second, samples are exposed to dried or moist air at two temperatures for up to 300 days in order to separate the effects of temperature and humidity in aging. In particular, it will be checked if a higher temperature only accelerates aging (as intended by conventional aging tests) or if the aging mechanisms are changed.

In addition, the chemical modifications are studied locally in order to get a better idea of the depth profiles of chemical aging. As surface-sensitive techniques like XPS, TOF-SIMS, or FTIR ATR spectroscopy are not suited to record depth profiles directly for a wide depth range, a low angle microtomy preparation technique has been established in previous work [16]. For the exposed surface zone, the depth profiles in an epoxy network are revealed by FTIR microspectroscopy on the cut face.

EXPERIMENTAL

The examined epoxy system consists of the diglycidyl ether of bisphenol A (DGEBA, D.E.R. 332 DOW Chemicals, Stade, Germany) and the aliphatic curing agent diethylene triamine (DETA, Fluka, Darmstadt, Germany). At room temperature, oxirane rings of DGEBA and primary or secondary amine groups of DETA react in a polyaddition to hydroxyl groups and secondary or tertiary amine groups, respectively. The stoichiometric ratio of oxirane rings and reactive amino hydrogen atoms corresponds to a mass ratio of DGEBA:DETA = 100:12 ("EP12"). Here, all oxirane rings and all amine groups are converted into hydroxyl groups and tertiary amines at full conversion. Additionally, samples with mass ratios of 100:10 ("EP10"), 100:14 ("EP14"), and 100:18 ("EP18") are prepared in order to study if remaining amine and oxirane groups might be attacked by aging reactions. The presence of such residual functional groups in the fully cured network is proved by near-infrared (NIR) transmission spectroscopy (IFS 66v/s with InSb detector, Bruker, Ettlingen, Germany) for post-cured bulk samples (thickness: 500 μm) with varying DETA content.

To produce bulk samples, the liquid monomers are stirred in the chosen mass ratio at 55°C for 5 min. Then, for room temperature (RT) curing (72 h) in CO_2-reduced, dried air (dew point: -70°C, residual CO_2 content: $\leq$200–300 ppm), the mixture is cast into a silicone mould placed on a PTFE film. The chemical conversion of epoxy rings is incomplete, but constant across the thickness of these RT-cured bulk samples [16]. Sample formation is finished by a post-curing step (argon atmosphere, 120°C, 1 h).

Samples are exposed to three environmental conditions: dried air at 120°C for 200 days or dried air or moist air (90% rel. humidity) at 60°C for 300 days. The surface to air is cut at a low angle by ultra microtomy (Ultra Cut E microtome, Reichert, Vienna, Austria) with diamond knives (Diatome, Biel, Switzerland) [16]. The chemical depth profile of the sample is studied point by point on the cut surface along a line scan from the cut edge at the sample surface to air into the bulk. At each position, an IR spectrum is recorded with a Bruker Hyperion 2000 FTIR-microscope in Attenuated Total Reflection mode (μ-ATR) in dried air. The lateral distance, l, on the cut surface corresponds to a depth $z = l \cdot \sin\alpha$ below the initial surface. Accordingly, a lateral resolution of 100 μm (= tip diameter of the germanium ATR crystal) corresponds to a depth resolution of 3.5 µm for the chosen angle $\alpha = 2°$. The exact cutting angle, α, between the surface to air and the cut surface is determined with a white light interferometer (New View 200, Zygo Corp., Middlefield, CT, USA). Unless noted otherwise, IR bands are assigned to chemical groups according to [17].

RESULTS AND DISCUSSION

Residual Reactive Groups in Post-Cured Epoxy Bulk

NIR-spectra of post-cured epoxy bulk samples with varying DETA content are shown in Figure 1. Bands are assigned according to [18]. Residual oxirane rings are visible at 4530 cm^{-1} only in EP10 due to the deficit of hardener. In EP12–EP18, no more oxirane is seen as enough amino hydrogen is available for post-curing. Primary amines (4935 cm^{-1}) are found only in EP18 due to the large excess of hardener. The band at 6475 cm^{-1} in EP18 is attributed to primary (6535 cm^{-1}) and secondary (6470 cm^{-1}) amine groups. In EP14, the lack of absorbance at 4935 cm^{-1} (primary amine) indicates that the combination band at 6475 cm^{-1} is dominated by secondary amines. In the stoichiometric EP12, neither oxirane nor amine groups are detected. Hence, the majority of oxirane and amine groups reacted with hydroxyl groups and tertiary amines. Due to steric hindrance

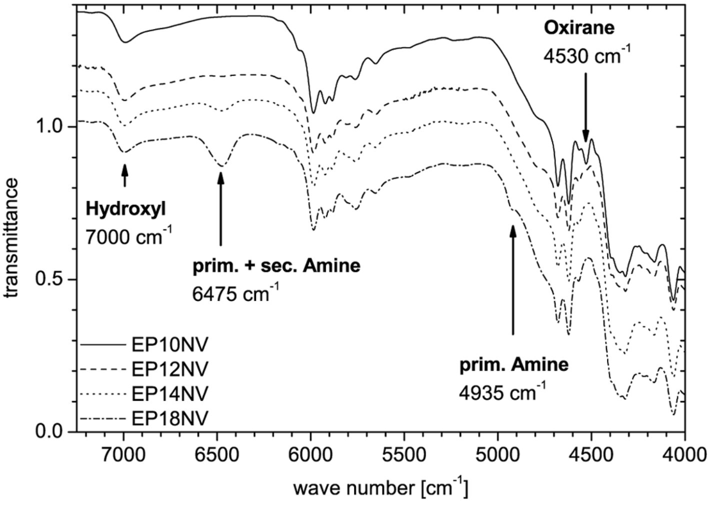

FIGURE 1 NIR-spectra (shifted in parallel) of post-cured epoxy bulk samples (EP10NV–EP18NV) with varying DETA content.

in the dense epoxy network, it is likely that some of the reacting groups are left. They are not seen since the sensitivity of NIR spectroscopy is limited. However, in MIR spectra the corresponding small band at 915 cm^{-1} is found in EP10–EP14 (not shown).

Moreover, MIR ATR microspectra on the cut surfaces of freshly prepared samples show no spatial dependence at all. Therefore, the epoxy samples can be considered as homogeneous for the given level of spatial resolution.

With a grain of salt, we suggest that, post-curing leads to a chemically completed network by either full oxirane conversion (EP12–EP18) or full amine conversion (EP10, EP12). Significant amounts of oxirane rings (EP10), primary (EP18), and secondary amines (EP14, EP18) remain in the cured network for the non-stoichiometric systems, while only a few of these groups remain in the stoichiometric bulk.

Aging in Dried Air at 120°C

As a starting point, Figure 2 depicts the spectra recorded on the surface of epoxy bulk samples (EP10–EP18) and in a depth of 350 μm after 25 days of aging in dried air at 120°C. The most pronounced changes in band intensity are marked by arrows. On the surface region to air, the broad O–H stretching vibration widens and shifts by *ca.* 100 cm^{-1}

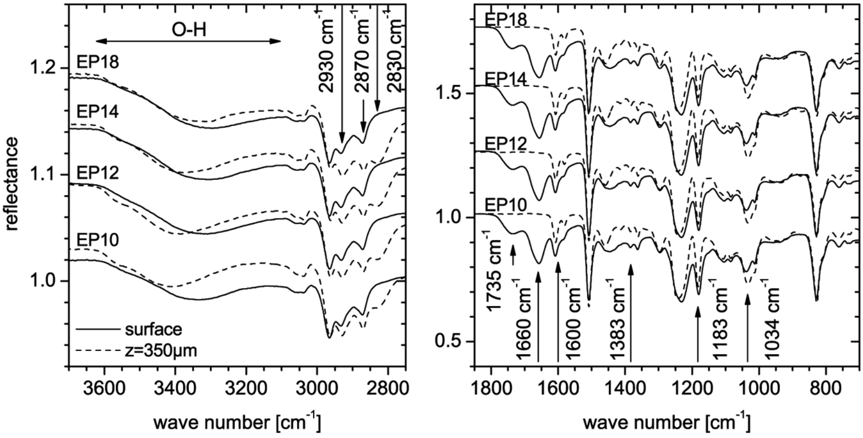

FIGURE 2 μ-ATR-spectra of EP10–EP18 after 25 days of aging in dried air at 120°C on the sample surface and in a depth z = 350 μm. Spectra are shifted vertically to ease inspection.

to smaller wave numbers. This indicates the formation of new hydroxyl or amine species. The C–H stretching vibrations at $2930\,\mathrm{cm}^{-1}$ and $2870\,\mathrm{cm}^{-1}$ lose intensity. They are attributed to methylene groups in the α-position to the phenylene ether [19]. Accordingly, the ether stretching vibration at $1034\,\mathrm{cm}^{-1}$ decreases as well [19]. The band at $2830\,\mathrm{cm}^{-1}$ that is assigned to methylene groups in the α-position to tertiary amines [19] even vanishes. New bands form at $1735\,\mathrm{cm}^{-1}$ and $1660\,\mathrm{cm}^{-1}$. Moreover, bands grow in the background at $1600\,\mathrm{cm}^{-1}$, $1383\,\mathrm{cm}^{-1}$, and $1183\,\mathrm{cm}^{-1}$. They have to be assigned to new chemical species.

All these spectral changes are fingerprints of the corresponding chemical aging reactions at the epoxy network.

The second key for the identification of the aging reactions is provided by the evolution of the band intensity profiles across the sample with aging time.

These depth profiles are derived for all aging-sensitive bands from their intensities $I_{\tilde{v}}(z)$ that are measured at each position z as the peak height with respect to a linear base line which is the same in all spectra for the given IR band. Deconvolution or band fitting are not applied. Normalization of $I_{\tilde{v}}(z)$ to the intensity of the phenyl band at $1510\,\mathrm{cm}^{-1}$ as an internal standard avoids interference from experimental effects like variations in the ATR contact area—Eq. (1):

$$I_{\tilde{v},\mathrm{norm}}(z) = \frac{I_{\tilde{v}}(z)}{I_{1510\,\mathrm{cm}^{-1}}(z)}. \tag{1}$$

Figure 3 provides an example for these depth profiles and compares $I_{\tilde{v},\mathrm{norm}}(z)$ after 25 days of aging at 120°C in dried air with the corresponding band intensities of the virgin samples that do not depend on z. For the aged state, all curves possess a sigmoid shape which is more or less well developed within a region of up to 200 µm in depth. This resembles the principal shape of a diffusion profile. On the bulk side, the intensities correspond to the virgin state before aging. At the edge to air, changes of the $I_{\tilde{v},\mathrm{norm}}(z)$ are strongest. Hence, permeating oxygen can be responsible for the observed chemical modifications from the surface towards the unaffected bulk.

For a given epoxy composition, the sigmoid shape and width of the gradient are not equal for all bands. There are bands showing a plateau close to $z = 0$ indicating that the reaction is close to full conversion in a surface zone. Others possess only a steep gradient in the surface region pointing at an earlier stage of reaction. Thus, the bands cannot

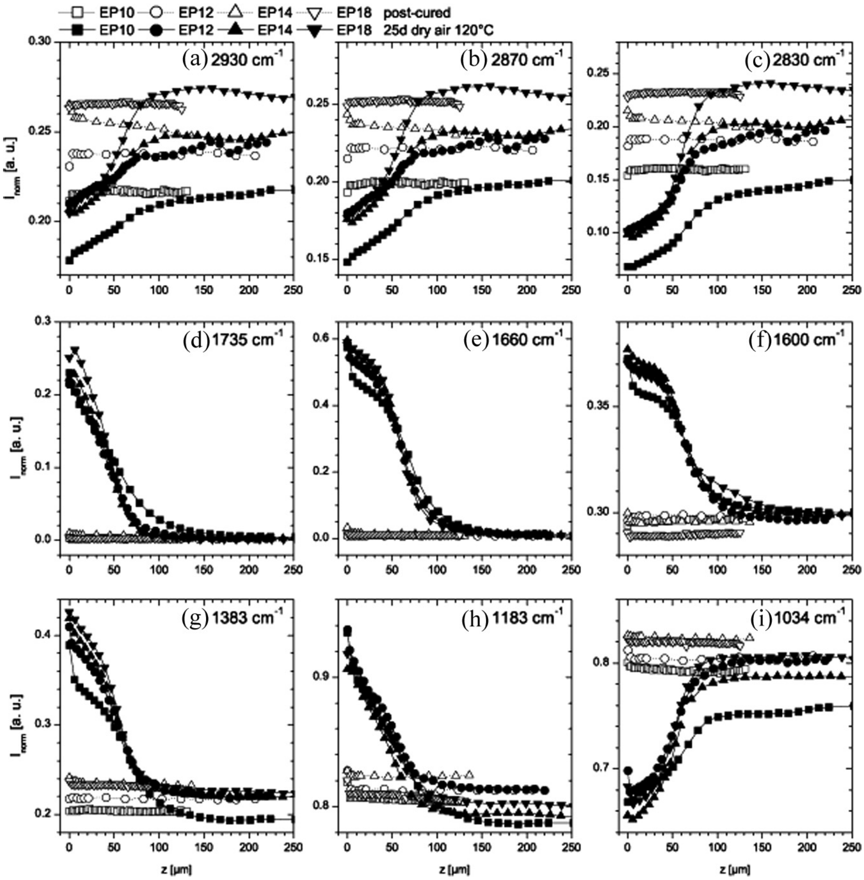

FIGURE 3 Depth profiles of aging-sensitive bands in the surface region of EP10–EP18 after 25 days of aging in dried air at 120°C.

result from a single chemical aging process. Bands with a similar depth profile should belong to the same chemical reaction or to the same product while deviating profiles indicate other reactions on a different time scale (At this point, it cannot be decided if these reactions proceed in parallel or as a sequence. For an answer, cf. discussion on chemical aging mechanisms below.)

For any given band, the profile step height and the values for $I_{\tilde{v},norm}(z \rightarrow 0)$ depend little on the monomer mixing ratio for EP12–EP18. However, EP10, with less than stochiometric content of amine, deviates systematically in one respect from the other networks of the other epoxies: step heights are smaller for almost any band of interest.

This indicates that aging does not affect the residual oxirane rings. It is the concentration of any kind of amine groups that plays the main role in the chemical aging reactions in dried air at 120°C. However, residual secondary amines in EP14 and EP18 do not notably influence the character of aging. Thus, all mechanisms should attack amines and other groups that are present in all networks but not the oxirane rings.

Prolonged aging up to 200 d just enhances the observed effects. No other spectral changes are found. With these findings, possible chemical aging mechanisms can be discussed.

In all mixtures, the polyaddition of epoxy rings and amines results in hydroxyl groups in the network. According to [6,20], part of these OH-groups could dehydrate during aging due to the high temperature resulting in water and alkene units which absorb at about 1660 cm^{-1}—Eq. (2):

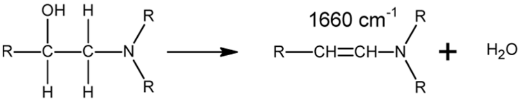

(2)

However, Reaction (2) cannot cause the observed intensity profile for that band since dehydration would proceed homogeneously inside the whole epoxy sample. As the alternative, the OH-groups in the network could oxidize with permeating oxygen to ketones (1735 cm^{-1})—Eq. (3):

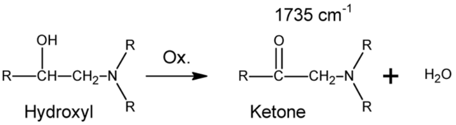

(3)

At a first glance, Reaction (3) would explain the spatial profiles for I_{1735} but it does not go with the increasing band intensity in the OH stretching region above 3100 cm^{-1}. Moreover, high temperature ($T > 300°C$) and catalysts are reported as prerequisites for quantitative ketone formation [21]. Thus, the oxidation of hydroxyl groups at best plays a minor role in aging at 120°C and at lower temperatures.

All networks contain tertiary amines as the crosslink in the network. They are reported to be oxidized by molecular oxygen to amine oxide that decomposes *via* Cope elimination at temperatures above 110°C [8,22,23]. Thus, the 120°C aging temperature is sufficient for that reaction. Equation (4) depicts the two options (i, ii) given for the oxidative cleavage of an amine crosslink:

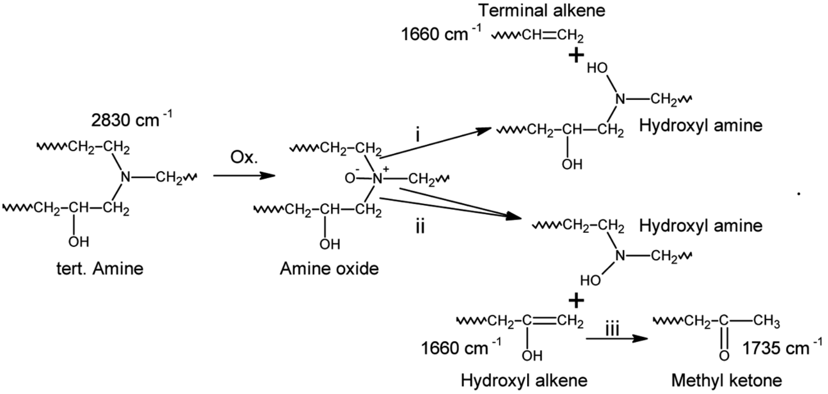 . (4)

This backbone scission weakens the epoxy network. Depending on which bond fails, it produces a hydroxyl amine (3300–3150 cm^{-1}) and either (i) a terminal C=C bond or (ii) a hydroxyl alkene group. Both possess a stretch vibration at *ca.* 1660 cm^{-1}. (iii) The hydroxyl alkene rearranges to a methyl ketone (1735 cm^{-1}) which is the more stable tautomer [8]. That sequence of reactions corresponds to changes observed in the IR spectra: the CH band intensity at 2830 cm^{-1} for the methylene groups in the α-position to tertiary amines decreases and the C=C and C=O stretching bands appear at 1660 cm^{-1} and 1735 cm^{-1}, respectively. Furthermore, the hydroxyl amine (3300–3150 cm^{-1}) may attribute to the OH band shift (*cf.* Fig. 2).

Due to the instability of the hydroxyl amine a sequence of parallel reactions follows—*cf.* Eq. (5) [8]:

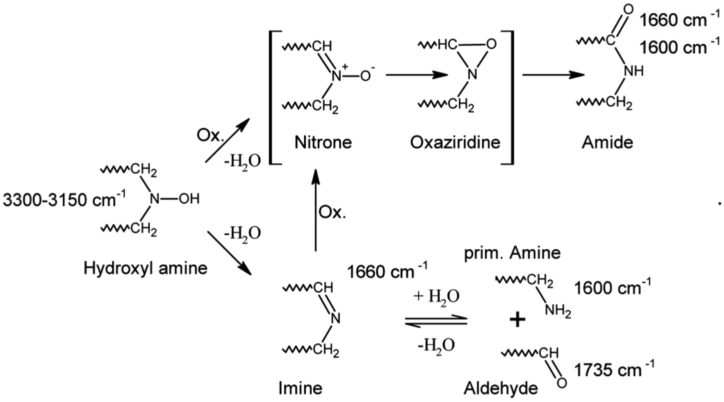 . (5)

The hydroxyl amine is either oxidized to an amide group (at *ca.* 1660 cm^{-1} and 1600 cm^{-1}) *via* unstable nitrone and oxaziridine intermediates [8,24,25] or it dehydrates to an imine (C=N, also at about 1660 cm^{-1}) that may be oxidized to yield an amide as well [8]. Alternatively, the *in situ* formed water can hydrolyze the imine into a primary amine and an aldehyde group. The primary amine contributes to the band shift at 3400–3000 cm^{-1} (*cf.* Fig. 2) and to the band at 1600 cm^{-1}. The aldehyde group provides intensity to the new band at 1735 cm^{-1} [22,23]. As all these products correspond to the observed aging bands, these reactions are possible in thermo-oxidative aging at 120°C.

Moreover, the reaction schemes (4,5) agree well with the depth profiles in Figure 3. The profiles $I_{\tilde{\nu},\mathrm{norm}}(z)$ for 2830 and 1660 cm^{-1} develop quite a plateau at $z \rightarrow 0$ while $I_{\tilde{\nu},\mathrm{norm}}(z)$ for 1735 cm^{-1} falls steeply in this region because it belongs to a product of a subsequent reaction.

C-atoms in α-position to tertiary amine groups as well to the ether group in the DGEBA entities are weak points of the epoxy network in a second respect because they are preferred sites for radical autoxidation with atmospheric O_2 [1–4,14,26]. Accordingly, autoxidation takes place either under UV irradiation at moderate temperatures or at 100–250°C in the dark. Thus, it could proceed at 120°C as illustrated in Eq. (6):

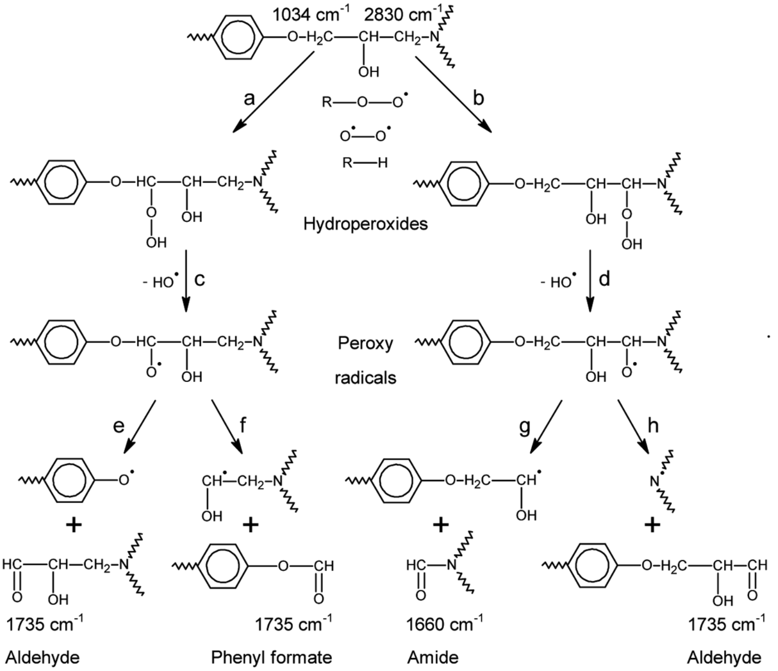

(6)

Methylene groups in α-position to amine (C−H stretch at $2830\,\text{cm}^{-1}$) and to ether groups (C−H stretch at $2928\,\text{cm}^{-1}$ [19]) are attacked by radicals (a, b) since their hydrogen atoms are easily abstracted. Accordingly, the band at $2830\,\text{cm}^{-1}$ vanishes while the band at $2930\,\text{cm}^{-1}$ decreases. The synchronous decline at $2870\,\text{cm}^{-1}$ might be due to the decrease of the neighbor bands. The resulting alkyl radicals add molecular oxygen to form peroxy radicals that can transfer their radical state to other methylene groups. The formed hydroperoxides absorb at 3560–$3530\,\text{cm}^{-1}$, but the band can be shifted due to hydrogen bonding to 3400–$3000\,\text{cm}^{-1}$ where an increase in absorption is observed. Additionally, the C−O stretching vibration of (hydro)peroxides might cause the increasing absorption at $1183\,\text{cm}^{-1}$. Thus, the autoxidative formation of hydroperoxides agrees well with the observed spectral changes.

As a subsequent reaction path, the formed hydroperoxides tend to dissociate into $OH^{\bullet}$ and peroxy radicals (c, d). The latter decompose and cleave the network (e–h) resulting in stable products such as aldehydes, (1735, $1383\,\text{cm}^{-1}$), amides (1660, $1600\,\text{cm}^{-1}$), and phenyl formiates ($1735\,\text{cm}^{-1}$). In consequence of network cleavage, the C-O-stretching band of ether groups at $1034\,\text{cm}^{-1}$ decreases. As the reactions e–h also produce radical species, consecutive reactions can create further products such as ketones (1735, $1383\,\text{cm}^{-1}$), peracids, and carboxylic acids [$1735\,\text{cm}^{-1}$, *cf.* Eq. (7)] and their salts (1600, $1383\,\text{cm}^{-1}$) [27].

These manifold products go well with the unusual width of the bands at 1735 and $1660\,\text{cm}^{-1}$.

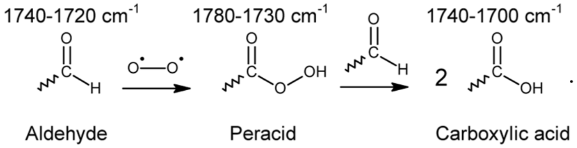 (7)

Radical autoxidation explains the development of *all* aging-sensitive IR bands (decrease of 2930, 2830, and $1034\,\text{cm}^{-1}$, increase of 3400–3000, 1735, 1660, 1600, 1383, and $1183\,\text{cm}^{-1}$). Additionally, it is the only mechanism that substantiates the consumption of ether groups. Thus, it can be concluded that autoxidation must proceed at 120°C. The Cope elimination described above is most likely to proceed at 120°C as well but we have no unequivocal spectroscopic evidence for that.

Now, it will be checked if the same mechanisms proceed at lower temperature.

Aging in Dried Air at 60°C

Figure 4 shows spectra of epoxy bulk (EP10–EP18) recorded on the sample surface and at a depth of 350 μm after 300 days of aging in dried air at 60°C. The changes in band intensity are less pronounced than at 120°C due to the expected slower reaction rates. Only 2830, 1660, 1600, and 1383 cm^{-1} are notably affected. Instead of 1735 cm^{-1}, however, a new band arises at 1725 cm^{-1} at 60°C. Additionally, most bands depend on the hardener content. Thus, the change in temperature does not only affect the aging kinetics. The depth profiles of those bands that are aging-sensitive at 60°C are depicted in Figure 5.

Now, the C–H stretching vibrations at 2930 and 2870 cm^{-1} do not change during aging except for EP18. Here, the band intensities show a concave gradient. 2830 cm^{-1} shows a gradient in all systems at 60°C. It is strong in EP18. Hence, the attack on residual primary or secondary amines might contribute to the band changes.

The other band profiles are convex gradients falling towards the bulk without constant levels or maxima. The band at 1034 cm^{-1} does not change intensity.

The newly growing band at 1725 cm^{-1} replaces the band observed at 1735 cm^{-1} for 120°C and it behaves differently. This indicates temperature-dependent variations of the chemical aging mechanisms. The gradient of the band at 1725 cm^{-1} is much weaker, it does not

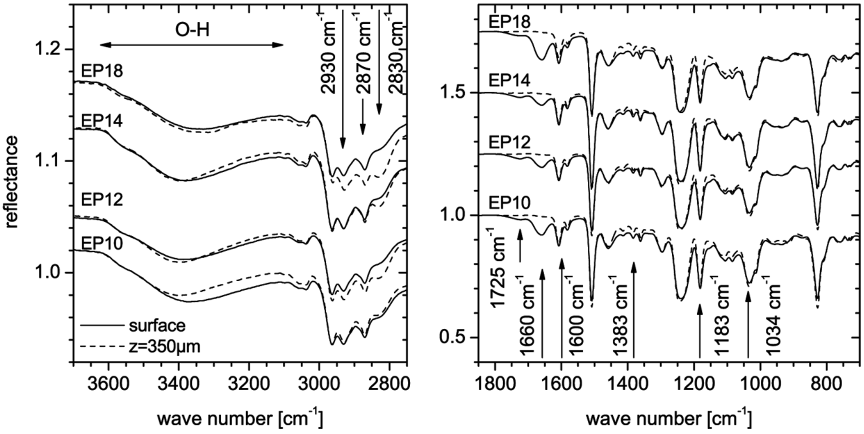

FIGURE 4 μ-ATR-spectra EP10–EP18 after 300 days of aging in dried air at 60°C on the sample surface and in a depth z = 350 μm.

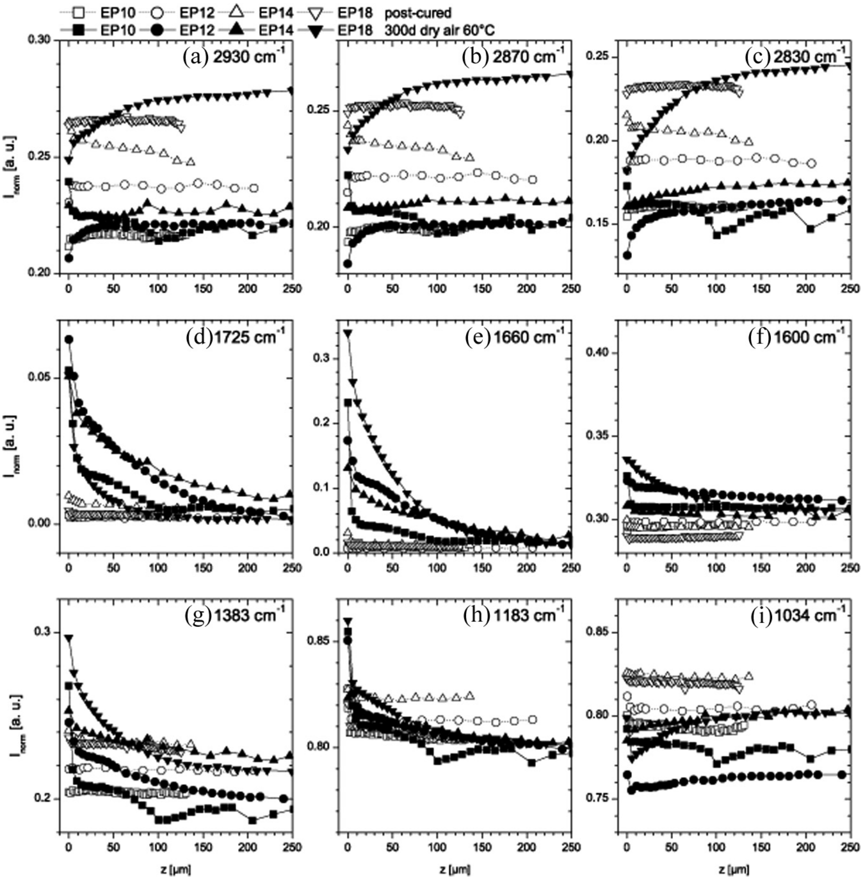

FIGURE 5 Depth profile of aging-sensitive bands in the surface region of EP10–EP18 after 300 days of aging in dried air at 60°C.

correlate with $1183\,\mathrm{cm}^{-1}$, and it depends on the monomer mixing ratio. In fact, $1725\,\mathrm{cm}^{-1}$ is strongest for EP12 and EP14 that are closest to the stoichiometric composition with the highest density of crosslinks. This result is pointing at a decomposition of network nodes.

1660, 1600, 1383, and $1183\,\mathrm{cm}^{-1}$ have similar, convex gradients. The bands also appear in EP10 and EP12 without excess of amine but their profiles become significantly higher and wider with increasing excess of amine. Hence, their formation is clearly favored by the presence of primary and secondary amines.

Based on these findings, changes and modifications in the chemical aging mechanisms are discussed.

The band development in EP10 and EP12 resembles aging at 120°C where tertiary amines and CH_2 groups in the α-position are attacked. In fact, both systems contain no significant amounts of other groups that might react. The oxidation by molecular oxygen is also observed at room temperature [20]. In addition, the time period studied here is much longer than in the cited works. Thus, the small aging effects in systems without amine excess are due to both autoxidation and Cope elimination. However, the carbonyl species formed at 120°C ($1735\,cm^{-1}$) and 60°C ($1725\,cm^{-1}$), respectively, are different. The hierarchy of reactions shown in Eqs. (4)–(6) is changed and/or the carbonyls are not further oxidized according to Eq. (7) under the mild condition of 60°C. Hence, not only kinetics, but also the chemistry changes with aging temperature.

Logically, radical autoxidation of α-CH_2 and oxidation of tertiary amines will also contribute to aging at 60°C in epoxies with excess of amine. However, the dependence of many bands on the DETA content suggests that they are not the only relevant chemical aging mechanisms at 60°C. EP14 and EP18 start with more amino hydrogen than epoxy rings, and hence primary and secondary amines remain in these fully cured samples. They can be involved in aging at 60°C as it is discussed now.

Primary amines are proven to be present in EP18. They are oxidized to hydroxylamine [28] which is unstable above 0°C, and hence oxidation proceeds to oximes ($1660\,cm^{-1}$)—Eq. (8). Accordingly, the band at $2830\,cm^{-1}$ of α-methylene groups at amines decreases. The resulting hydroxyl groups contribute to the shift and increase of the OH-band (cf. Figure 4) and to the band at $1383\,cm^{-1}$. A further oxidation of oxime to hydroxamic acid as shown in Eq. (8) can be excluded since no shift of the band at $1660\,cm^{-1}$ is observed. Now, the rise of 1660 and $1383\,cm^{-1}$ and the decrease of $2830\,cm^{-1}$ are most intense in EP18. Therefore, the oxidation of primary amines to oximes notably contributes to their band development.

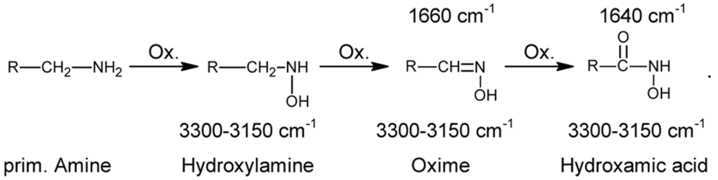

$$R{-}CH_2{-}NH_2 \xrightarrow{Ox.} R{-}CH_2{-}\underset{OH}{\underset{|}{NH}} \xrightarrow{Ox.} R{-}CH{=}\underset{OH}{\underset{|}{N}} \xrightarrow{Ox.} R{-}\overset{O}{\overset{\|}{C}}{-}\underset{OH}{\underset{|}{NH}}\ . \tag{8}$$

Secondary amine groups in EP14 and EP18 also can be oxidized to another hydroxylamine according to Eq. (9):

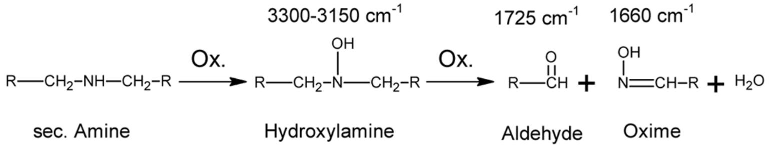

(9)

That reaction might also contribute to the increase and shift of the OH-band (*cf.* Fig. 4) because it is more stable than the hydroxylamine in Eq. (8). Nevertheless, it can be consecutively oxidized to oximes ($1660\,cm^{-1}$) and aldehydes ($1725\,cm^{-1}$)—Eq. (9) [28]. In the network, this oxidation is accompanied by backbone scissioning. This also explains why the decrease of $2830\,cm^{-1}$ becomes more pronounced with increasing hardener content.

The picture is not complete, however, because I_{1725} and I_{1660} do not develop synchronously. Hence, the reaction routes for hydroxylamines must be looked at in more detail. The combination of Eqs. (4), (8), and (9) results in

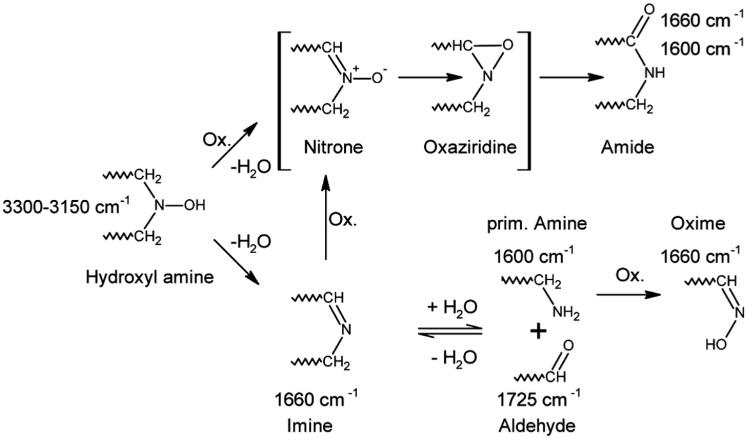

(10)

Accordingly, the formation of amide groups (1660 and $1600\,cm^{-1}$) or the decomposition into an aldehyde ($1725\,cm^{-1}$) and a primary amine ($1600\,cm^{-1}$) are possible. In the literature, both reactions are discussed as consecutive reactions of Cope elimination at elevated temperature (see above), but may also proceed slowly at 60°C. A subsequent oxidation of the formed primary amine ($1600\,cm^{-1}$) according to Eq. (8) may complete the oxidation of hydroxyl amines to aldehydes ($1725\,cm^{-1}$) and oximes ($1660\,cm^{-1}$) according to Eq. (4). This more detailed view is supported by the observation that most changes of the involved aging-sensitive bands (2830, 1660, 1600, 1383 cm^{-1}) are more pronounced at 60°C if more residual secondary amines are present. They are an additional source for the formation of hydroxylamines and their known consecutive reactions. Furthermore, intensities of 1725 and 1660 cm^{-1} need not correlate strictly anymore. Thus, the oxidation of secondary amines is likely to proceed as a sequence of reactions.

In parallel, some of the formed carbonyls according to Eqs. (4)–(6), and (10) can react with residual secondary amine groups to enamines (1660 cm^{-1})—*cf.* Eq. (11):

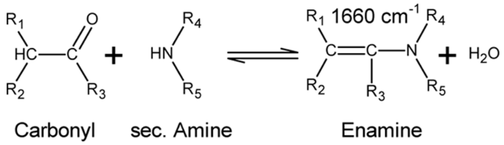

(11)

This reaction will also contribute to 1660 cm^{-1}. Its presence is supported by the observed inverse dependence of I_{1725} on the DETA content. First, the reaction of carbonyls formed during the oxidation of secondary amines with another secondary amine explains why I_{1725} and I_{1660} do not develop synchronously at 60°C. Second, the more secondary amines are present in the network, the more carbonyls are consumed. Thus, the gradient of I_{1725} is smaller at higher amine excess while I_{1660} becomes stronger. However, no temporal decrease of I_{1725} is observed. Therefore, the consumption of carbonyl groups is slower than their formation. This is reasonable because both species are integrated into the network. Thus, their reaction depends on their encounter which is limited by the low molecular mobility.

In conclusion, the oxidation of primary and secondary amines and the subsequent reaction of carbonyls with secondary amines to enamines are important additional aging mechanisms at 60°C for systems with excess content of hardener. In all other systems autoxidation of α-CH_2 at amine and phenylether entities and the oxidation of tertiary amines are the only aging mechanisms. They proceed slowly and produce products different from those found at 120°C.

Thus, a change of aging temperature does not change the proceeding mechanisms in general. As the kinetics of any chemical reaction depend on temperature in a specific way, their ranking and, thus, the character of aging changes when temperature is varied. *Hence, lifetime predictions based only on "accelerated" aging tests at higher temperature might lead to false results.*

Aging in Moist Air at 60°C

Spectra of epoxy bulk samples (EP10–EP18) recorded on the surface and at a depth of 350 μm after 300 days of aging in moist air at 60°C are given in Figure 6.

Impact is seen on the same bands as for aging in dried air, except for 1725 cm^{-1} that does not appear. Again, many bands depend on the hardener content but their quantitative changes differ between dried and moist air. Figure 7 depicts depth profiles of aging-sensitive bands.

In Figure 7, the C–H stretching vibrations at 2930, 2870, and 2830 cm^{-1} do not change systematically except for EP18 where the bands decrease in a surface region.

The rise of 1725 cm^{-1} is almost completely suppressed. This band is reduced to a small and weak gradient over 50 μm. Thus, water hinders the formation of carbonyls or initiates their conversion. Likewise, the bands at 1183 and 1034 cm^{-1} show weak convex gradients over 50 μm. Spectra indicate that these variations are negligible.

The bands at 1660, 1600, and 1383 cm^{-1} clearly increase with the amine content. Hence, residual primary and secondary amines are involved in their formation under moist air.

1600 cm^{-1} shows a maximum at a depth of 50 μm under the surface indicating the loss or further conversion of the corresponding aging products. Note that the band reaches higher intensity at 60°C in moist air than at 120°C in dried air. Obviously, water accelerates its formation even more than elevated temperature.

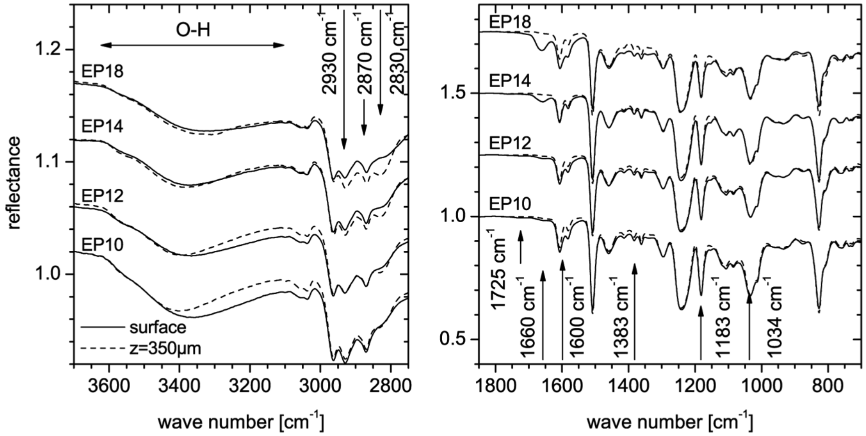

FIGURE 6 μ-ATR-spectra EP10–EP18 after 300 days of aging in moist air at 60°C on the sample surface and in a depth z = 350 μm.

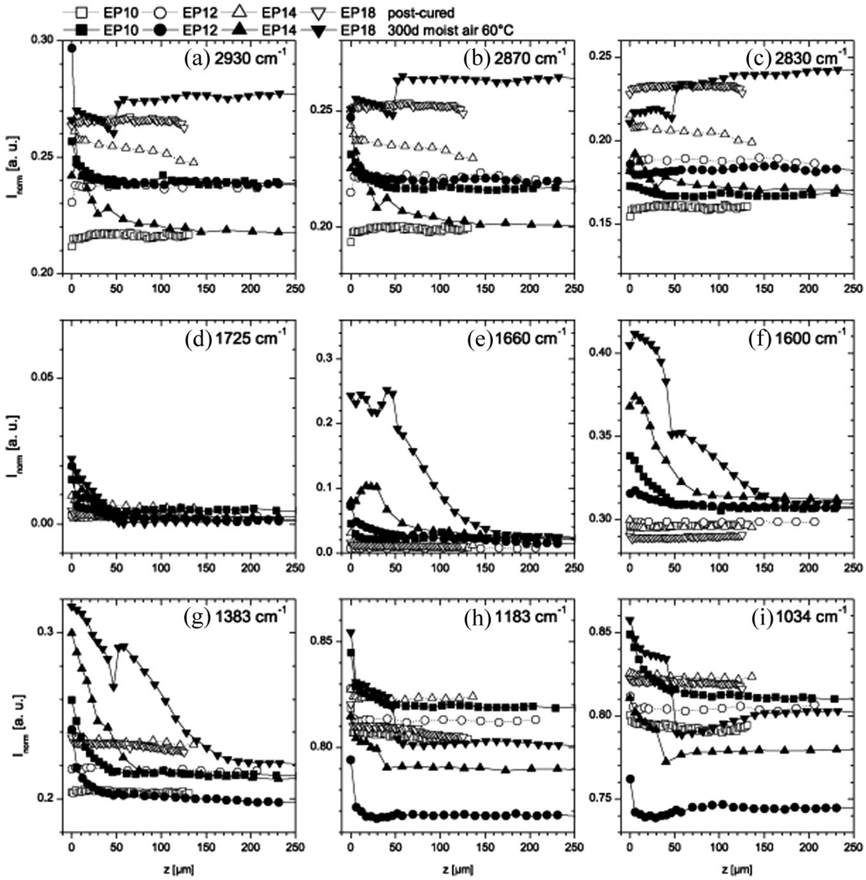

FIGURE 7 Depth profile of aging-sensitive bands in the surface region of EP10–EP18 after 300 days of aging in moist air at 60°C.

The comparable intensities and the dependence of most bands on the DETA content under dry and moist conditions suggest that the penetrating water does not completely change the chemical aging mechanisms. Nevertheless, several peculiarities have to be considered in detail.

In moist air, water plasticizes the stiff epoxy network and lowers the glass transition temperature from 131 to 99°C in the post-cured EP14 bulk [6]. Plasticization enhances any macromolecular mobility and molecular diffusion processes. That will accelerate the reactions that proceed under dry aging conditions. Furthermore, the influence of water on the equilibrium of the reactions and its reaction with the aging products has to be considered. Additionally, water molecules accumulate at polar groups of the network like amines and hamper their oxidation by protonation.

Water strongly favors the formation of the intensity gradient for the band at 1600 cm^{-1} at higher DETA contents. Chemical degradation by water is not the reason for that since water penetrates the whole sample before aging becomes detectable [6]. Also, the gradient cannot result directly from a partial protonation of secondary and tertiary amine groups since it affects the whole sample as well. However, the hydrolysis of imines to amine groups (1600 cm^{-1}) after Cope elimination or after oxidation of secondary amines [Eq. (5)] is favored under moist conditions due to the excess of water. Additionally, a partial protonation of the formed primary amines [Eq. (5)] by water hinders their oxidation and enhances their absorption. This can explain the stronger band at 1600 cm^{-1} under moist conditions.

The band at 1725 cm^{-1} develops much weaker in moist air. First, the formation of carbonyl species [Eqs. (4)–(6) and (10)] may be hampered due to a partial protonation of secondary and tertiary amine groups. That would slow down their oxidation. Second, the plasticization of the network by water facilitates the reaction of carbonyls with secondary amines to enamines [Eq. (11)]. Third, the hydrolysis of formed aldehydes to geminal diols (*e.g.*, 58% conversion in the case of aqueous solution of acetaldehyde [29]) also reduces I_{1725} under moist conditions as in Eq. (12).

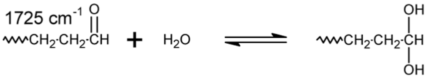

$$\overset{1725\ \text{cm}^{-1}}{\sim\!\sim CH_2{\cdot}CH_2{\cdot}\overset{\overset{O}{\|}}{C}H} + H_2O \rightleftharpoons \sim\!\sim CH_2{\cdot}CH_2{\cdot}\underset{OH}{\overset{OH}{C}}H \qquad (12)$$

Logically, a maximum in peak intensity as for for the bands at 1660 and 1600 cm^{-1} is due to a maximum of concentration of the corresponding chemical species. It reflects competing processes of formation and consumption or removal. The plasticization of the network enhances any molecular mobility. Thus, volatile network fragments can diffuse more easily to the surface and evaporate under dry conditions leading to the depletion zone. In fact, such short fragments have been found with ESI in the immersion bath of epoxy bulk samples aged at 60°C [6].

CONCLUSIONS

The aging of DGEBA-DETA epoxy adhesives in the surface region of the bulk material was studied with FTIR ATR microspectroscopy on sample surfaces prepared with low angle microtomy. The role of temperature and humidity in aging was separated by three environmental conditions: dried air or moist air (90% rel. humidity) at 60°C or dried air at 120°C for up to 300 days. This approach allows the investigation of the affected region locally, to determine its thickness and to discriminate depth profiles of IR bands.

Spectral changes are found in a gradient region of up to more than 200 µm in depth. They monitor thermo-oxidative modifications that start at the bulk surface and advance into the material. Their kinetics is controlled by the diffusion of atmospheric oxygen and water within the polymer. The spectral changes can be correlated to the formation of new species such as carbonyl groups (1725 and 1735 cm^{-1}), oximes, amides, enamines, and alkenes (1660 cm^{-1}) and amides, primary amines, or carboxylic acid salts (1600 cm^{1}). The intensity and depth profile of the aging-sensitive bands depend in a complex way on temperature, humidity, and the epoxy-amine stoichiometry. On that basis, the following reaction mechanisms are deduced.

At 120°C, autoxidative attack on methylene in the α-position to tertiary amines and to phenylene ether followed by hydroperoxide decomposition result in carbonyl and amide groups and chain scissions in accordance with [1,2,4,12]. Additionally, tertiary amine groups are oxidized and then cracked by Cope elimination followed by hydroxylamine decomposition [8]. Hence, several chemical aging mechanisms proceed in parallel *via* cascades of chemical reactions. Both hydroperoxide decomposition and Cope elimination result in the scission of network nodes that weakens the network.

Both mechanisms proceed slowly at 60°C as well, but other products than those at 120°C dominate. Furthermore, the oxidation of residual primary and secondary amines and the consecutive reaction of the formed carbonyls with secondary amines to enamines enhance aging significantly at 60°C for systems with an excess of hardener. These reactions should also proceed at 120°C but we found no spectroscopic evidence for them. Obviously, their effects are surpassed by far by autoxidation of α-CH_2 and oxidation of tertiary amines. This result illustrates how strongly temperature affects the kinetics of the reactions and, thus, their hierarchy.

Humidity affects the equilibrium of several reactions, thus, altering some band intensities. A principal change of the chemical mechanisms is not identified. Additionally, water favors the loss of small network fragments as it plasticizes the network. For a dicyandiamide cured epoxy which forms another network than that in the DGEBA-DETA system, such a network damage with subsequent leaching of degradation products was deduced by De Neve and Shanahan [30] from gravimetric data obtained at moderate temperatures (40–70°C) in aging experiments that lasted up to 2 years.

With all the deduced reactions in mind, it should be noticed that the gradients for the different band intensities observed as a function of aging time do not directly relate to the diffusion of oxygen or water into the epoxy. They rather depict resulting chemical changes with their own kinetics, and in some cases several of these reactions contribute to a given band intensity. Hence, it makes no sense to calculate formally the diffusion constants from the observed intensity gradients.

The observed evolution of various chemical gradients across some hundred microns during aging does result in changes of the mechanical properties of the DGEBA-DETA epoxy networks in a corresponding mechanical interphase [31]. This conclusion is very relevant to applications and testing of epoxy networks on the microscale, *e.g.*, for the microbond test with little drops of cured resin on fibers for composites [32–34]. So far, the finite element analysis for the test allows for an interphase at the epoxy-fiber contact in an otherwise homogeneous epoxy. A mechanical interphase at the contact with air due to aging implies that an advanced model is needed.

From a more general point of view, our results show that the long-term aging behavior at moderate temperature cannot be predicted safely from aging tests at higher temperature alone. As the consequence, these short-term aging tests cannot replace the aging under application conditions. However, the short-term tests can be used to identify the chemical aging mechanisms and to select those which are harmful to the epoxy network. This chemical knowledge can be then, in principle, be utilized to identify critical environmental conditions and to modify the epoxy composition in order to reduce or even avoid critical aging processes.

REFERENCES

[1] Damian, C., Espuche, E., and Escoubes, M., *Polym. Degrad. Stab.* **72**, 447–458 (2001).

[2] Bellenger, V. and Verdu, J., *J. Appl. Polym. Sci.* **30**, 363–374 (1985).

[3] Colin, X., Marais, C., and Verdu, J., *Polym. Test.* **20**, 795–803 (2001).

[4] Luoma, G. A. and Rowland, R. D., *J. Appl. Polym. Sci.* **32**, 5777–5790 (1986).

[5] Fata, D. and Possart, W., *J. Appl. Polym. Sci.* **99**, 2726–2736 (2006).

[6] Bockenheimer, C., Fata, D., and Possart, W., *J. Appl. Polym. Sci.* **91**, 369–377 (2004).

[7] Bockenheimer, C., Fata, D., and Possart, W., *J. Appl. Polym. Sci.* **91**, 361–368 (2004).

[8] Burton, L. B., *J. Appl. Polym. Sci.* **47**, 1821–1837 (1993).

[9] Zhang, G., Pitt, W. G., Goates, S. R., and Owen, N. L., *J. Appl. Polym. Sci.* **54**, 419–427 (1994).

[10] Monney, L., Dubois, C., and Chambaudet, A., *Angew. Makromol. Chem.* **273**, 6–11 (1999).

[11] Rivaton, A., Moreau, L., and Gardette, J. L., *Polym. Degrad. Stab.* **58**, 321–332 (1997).

[12] Rivaton, A., Moreau, L., and Gardette, J. L., *Polym. Degrad. Stab.* **58**, 333–339 (1997).

[13] Barral, L., Cano, J., López, J., López-Bueno, I., Nogueira, P., Abad, M. J., and Ramírez, C., *Eur. Polym. J.* **36**, 1231–1240 (2000).

[14] Buch, X. and Shanahan, M. E. R., *J. Appl. Polym. Sci.* **76**, 987–992 (2000).

[15] Fata, D., *Epoxidsysteme im Verbund mit rostfreien Stählen – Vernetzung und Alterung (Epoxy systems in contact with stainless steel – curing and aging)*, Saarbruecker Reihe Materialwissenschaft und Werkstoffechnik, vol. 9, Shaker Verlag, Aachen, Germany, 2007.

[16] Meiser, A., Willstrand, K., Fehling, P., and Possart, W., *J. Adhes.* **84**, 299–321 (2008).

[17] Socrates, G., *Infrared amd Raman Characteristic Group Frequencies — Tables and Charts*, (John Wiley & Sons, Chichester, 2004), 3rd ed.

[18] Siesler, H. W., Ozaki, Y., Kawata, S., and Heise, H. M., *Near-Infrared Spectroscopy-Principles, Instruments, Applications*, (Wiley-VCH, Weinheim, 2001), 1st ed.

[19] Wehlack, C., *Chemische Struktur und ihre Entstehung in dünnen Epoxid- und Polyurethanschichten auf Metallen*, (Chemical structure and its formation in thin epoxy and polyurethane layers on metals) Saarbrücker Reihe Materialwissenschaft und Werkstofftechnik, (Shaker Verlag, Aachen, 2009), Vol. 14.

[20] Pascault, J.-P., Sautereau, H., Verdu, J., and Williams, R. J. J., *Thermosetting Polymers*, (Dekker, New York, 2002), ISBN 0-8247-0670-6, p. 460.

[21] Becker, H. G. O., *Organikum*, (VEB Verlag der Wissenschaften, Berlin, 1988), 17th ed.

[22] Latscha, H. P., Kazmaier, U., and Klein, H. A., *Organische Chemie – Chemie-Basiswissen II*, (Springer, Berlin, 2002), 5th ed.

[23] Freytag, H., Möller, F., Pieper, G., and Söll, H., Umwandlung von Aminen, in *Methoden der organischen Chemie* (Houben-Weyl), Band XI/2: Stickstoffverbindungen II, E. Müller (Ed.) (Georg Thieme Verlag, Stuttgart, 1957).

[24] Hamer, J. and Macaluso, A., *Chemical Reviews* **64**, 473–495 (1964).

[25] Lamchen, M., Nitrone rearrangements, in *Mechanisms of Molecular Migrations*, (Interscience, New York, 1968).

[26] Buch, X. and Shanahan, M. E. R., *Polym. Degrad. Stab.* **68**, 103–411 (2000).

[27] Becker, H. G. O., *Organikum*, (Johann Ambrosius Barth Verlag, Heidelberg, 1996), 20th ed.

[28] Metzger, H., Oxime, in *Methoden der organischen Chemie* (Houben-Weyl), Band XI/1: Stickstoffverbindungen II, E. Müller (Ed.) (Georg Thieme Verlag, Stuttgart, 1957).

[29] Bruice, P. Y., *Organische Chemie*, (Pearson Studium, München, 2007).

[30] De Neve, B. and Shanahan, M. E. R., *J. Adhes.* **49**, 165–176 (1995).

[31] Meiser, A., unpublished data.

[32] Yamaki, J.-I. and Katayama, Y., *J. Appl. Polym. Sci.* **19**, 2897–2909 (1975).

[33] Carroll, B. J., *J. Colloid Interface Sci.* **57**, 488–495 (1976).

[34] Ash, J. T., Cross, W. M., Svalstad, D., Kellar, J. J., Kjerengtroen, L., *Composites Science and Technology* **63**, 641–651 (2003).